Published in final edited form as:
Sci Signal. ; 2(61): ra10. doi:10.1126/scisignal.2000162.

Rac1 Is a Critical Mediator of Endothelium-Derived Neurotrophic Activity

Naoki Sawada[1], **Hyung-Hwan Kim**[1], **Michael A. Moskowitz**[2], and **James K. Liao**[1,*]

1*Vascular Medicine Research, Brigham and Women's Hospital, 65 Landsdowne Street, Room 275, Cambridge, MA 02139, USA.*

2*Stroke and Neurovascular Regulation Laboratory, Massachusetts General Hospital, Charlestown, MA 02129, USA.*

Abstract

The therapeutic potential of neurotrophic factors has been hampered by their inability to achieve adequate tissue penetration. Brain blood vessels, however, could be an alternative target for neuro-salvage therapies by virtue of their close proximity to neurons. Here we show that hemizygous deletion of *Rac1* in mouse endothelial cells (ECs) attenuates brain injury and edema after focal cerebral ischemia. Microarray analysis of *Rac1*$^{+/-}$ ECs revealed enrichment of stress response genes, basement membrane components, and neurotrophic factors that could affect neuronal survival. Consistent with these expression profiles, endothelial *Rac1* hemizygosity enhanced antioxidative and endothelial barrier capacities and potentiated paracrine neuroprotective activities through the up-regulation of the neurotrophic factor, artemin. Endothelial Rac1, therefore, could be an important therapeutic target for promoting endothelial barrier integrity and neurotrophic activity.

INTRODUCTION

Vascular endothelial cells (ECs) are emerging targets for neuroprotection (1). For the maintenance of vascular integrity, ECs, together with the underlying basal lamina and astrocyte endfeet constitute the blood-brain barrier (BBB) (2). In the early phases of many neurological diseases and ischemic stroke, increased production of reactive oxygen species (ROS) and activation of proteases cause disruption of the BBB and transudation of plasma components. This leads to edema, which exacerbates neuronal damage (3). Therefore, protection of BBB integrity is an important component of neuroprotective therapies. The small guanosine triphosphatase (GTPase) Rac1 is a critical mediator of various aspects of EC function. In addition to its effects on gene expression, Rac1 regulates ROS production, endothelial

*To whom correspondence should be addressed. E-mail: jliao@rics.bwh.harvard.edu.

SUPPLEMENTARY MATERIALS
www.sciencesignaling.org/cgi/content/full/2/61/ra10/DC1
Materials and Methods
Supplementary Text
Fig. S1. CD31 labeling of *Rac1*$^{+/-}$ and *Rac1*$^{+/+}$ ECs.
Fig. S2. *Rac1*$^{+/-}$ ECs show retarded proliferation, migration, and capillary formation.
Fig. S3. CD31 labeling of MBECs.
Table S1. Representative gene sets enriched in *Rac1*$^{+/+}$ mouse ECs.
Table S2. Representative gene sets enriched in *Rac1*$^{+/-}$ mouse ECs.
Table S3. Transcription factors differentially expressed between *Rac1*$^{+/-}$ and *Rac1*$^{+/+}$ mouse ECs.
Table S4. List of differentially expressed genes between *Rac1*$^{+/-}$ and *Rac1*$^{+/+}$ mouse ECs.

Citation: N. Sawada, H.-H Kim, M. A. Moskowitz, J. K. Liao, *Rac1* is a critical mediator of endothelium-derived neurotrophic activity. *Sci. Signal*. **2**, ra10 (2009).

permeability, and cell adhesion (4–6), all of which have been implicated in the deterioration of neurovascular integrity in neurological diseases.

In animal studies, neurotrophic factors prevent the neuronal death associated with various neurological disorders. However, the efficacy of these agents in humans has been limited by their inability to penetrate target neural tissues, necessitating their invasive delivery (7–9). Emerging evidence suggests that neurons, glial cells, pericytes, and ECs, by virtue of their close proximity, form a topographical compartment termed the neurovascular unit, in which they are functionally coupled to maintain brain homeostasis (10,11). This functional coupling involves reciprocal trophic signaling. Indeed, recent evidence indicates that ECs can support neuronal survival through paracrine signals (12,13). Given the pharmacological accessibility of vascular endothelium in vivo, the exploitation of EC-derived neurotrophic activity could provide a feasible strategy for safe and efficacious neuroprotection. However, this approach has been hampered by the lack of information on the regulatory mechanisms that direct EC paracrine signaling and coordinate them with EC-mediated vascular functions. In this study, we tested the hypothesis that endothelial Rac1 provides a therapeutic target for promoting vascular integrity and neuronal survival.

RESULTS

Neuroprotection in endothelial *Rac1* haploinsufficient mice

To determine the endothelium-specific role of Rac1, we generated mice with conditional deletion of the *Rac1* gene in ECs (14). *Rac1* null mutation in ECs was achieved by crossing Tie2 promoter and enhancer-driven Cre Tg with *Rac1* floxed allele knock-in mice (15,16). Because EC-*Rac1* null homozygosity results in embryonic lethality, we used EC-*Rac1* haploinsufficient (EC-$Rac1^{+/-}$) and control ($Rac1^{flox/+}$) mice. The EC-$Rac1^{+/-}$ mice showed a 50% decrease in endothelial Rac1 protein abundance and activity; however, body and organ development was similar to that of control mice.

To investigate the effect of reducing endothelial Rac1 on neuroprotection, mice were subjected to 2-hour middle cerebral artery occlusion (MCAo) followed by 22-hour reperfusion, a model of acute nonthrombotic focal ischemia (Fig. 1A) (17). Infarct size, which reflects the extent of ischemic cell death, was 37% smaller in EC-$Rac1^{+/-}$ mice than in controls (Fig. 1B). Edema volume, which depends on BBB disruption, was 63% smaller in EC-$Rac1^{+/-}$ mice than in controls (Fig. 1C). Consistent with these anatomical findings, neurological deficits were less severe in EC-$Rac1^{+/-}$ mice than in control mice (Fig. 1D). Neuroprotection in the transient MCAo model is thought to depend on two major factors: residual cerebral blood flow (CBF) in the ischemic region and CBF-independent, direct neuroprotective components, such as BBB functionality and growth factor–mediated neurosurvival. The decrease in CBF in the ischemic hemisphere during MCAo was comparable in EC-$Rac1^{+/-}$ and control mice (Fig. 1E). Furthermore, the mean arterial blood pressure and blood gas profiles in the two groups were similar (Table 1).

Expression profiling of *Rac1* haploinsufficient ECs

The independence from differences in blood flow of the reduction of infarct size in EC-$Rac1^{+/-}$ mice compared to controls suggested that decreasing EC Rac1 had a direct neuroprotective effect. To explore this possibility, we performed a genome-wide microarray analysis in which we compared $Rac1^{+/-}$ and $Rac1^{+/+}$ mouseprimary ECs. The integrity of the EC preparation was verified by >98% PECAM-1 (platelet endothelial cell adhesion molecule 1)–positive labeling and the 50% reduction of total and active Rac1 abundance in $Rac1^{+/-}$ versus $Rac1^{+/+}$ ECs (Fig. 2A and fig. S1). Tetraplicate hybridizations on the Massachusetts General Hospital 19,549 oligo chips revealed differential expression of 299 gene features

(~1.5%) in *Rac1*$^{+/-}$ versus *Rac1*$^{+/+}$ ECs ($P < 0.05$, fold increase greater than 1.5 or less than −1.5) (Fig. 2, B and C, and table S4). To characterize the global features of these genes, we assessed functional annotation clustering of genes whose expression was down-regulated or up-regulated in *Rac1*$^{+/-}$ ECs (Fig. 2, D and E) (18). Additionally, the small but cumulatively significant difference in gene expression between *Rac1*$^{+/-}$ and *Rac1*$^{+/+}$ ECs across the whole array data was determined by enrichment of a priori–defined gene sets [gene set enrichment analysis (GSEA); false discovery rate <25%; see Supplementary Materials and Methods] (Fig. 2, F and G, and tables S1 and S2) (19). Quantitative reverse transcription polymerase chain reaction (qRT-PCR) analysis of selected genes showed a good correlation ($R = 0.859$) between the fold increase measured by microarray and that measured by qRT-PCR (Fig. 2, H and I). In addition, crystallin αB immunolabeling was more intense with *Rac1*$^{+/-}$ than with *Rac1*$^{+/+}$ ECs, consistent with the 4.24-fold up-regulation of the crystallin αB (*Cryab*) messenger RNA (mRNA) seen in the microarray data (Fig. 2J).

Functional clustering and GSEA revealed that many genes whose expression was decreased in *Rac1*$^{+/-}$ ECs are associated with mitotic cell division (Fig. 2, D and F, Supplementary text, Table 2, and tables S1 and S3). The expression of many of these genes is tightly controlled in a cell cycle–dependent fashion, suggesting that their down-regulation represents an overall growth-inhibitory state of *Rac1*$^{+/-}$ ECs. Indeed, *Rac1*$^{+/-}$ ECs exhibited decreased proliferation and capillary formation compared to *Rac1*$^{+/+}$ ECs (fig. S2A). These findings are consistent with the recognized roles of Rac1 in mediating cell cycle progression, further validating our microarray data (20).

Rac1$^{+/-}$ ECs show increased expression of gene clusters relevant to neurovascular protection

Functional clustering revealed enrichment of *Rac1*$^{+/-}$ ECs in three gene categories that were potentially relevant to their neurotrophic properties. There was increased expression of genes encoding proteins implicated in the stress response (“stress response genes”), genes encoding proteins associated with cell adhesion and the extracellular matrix (ECM) (“cell adhesion genes” and “ECM genes”), and genes encoding growth factors (Fig. 2E and Table 3). The functional relevance of these expression profiles was examined by testing appropriate cellular phenotypes (Figs. 3 to 5). The stress response genes included *Gpx3*, which encodes glutathione peroxidase 3 (Gpx3), an extracellular scavenger of ROS that catalyzes the reduction of hydrogen peroxide and lipid peroxides (21). Decreased Gpx3 activity is associated with familial child stroke (22). Up-regulated stress response genes also included those encoding three heat shock proteins (HSPs), crystallin αB, hsp25, and hsp70, which protect cells from apoptosis under various stress conditions (23–25). Various neurological diseases are associated with increased generation of ROS in the vascular wall, a process that both leads to the proteolytic disruption of the BBB and decreases neurovascular cell survival. EC death, in turn, causes further deterioration of BBB function. We therefore examined how *Rac1* haploinsufficiency affected the ROS-generating capacity of ECs in hypoxia-reoxygenation (H/R), a condition that mimics ischemia-reperfusion injury in MCAo. In *Rac1*$^{+/+}$ ECs, H/R elicited a 1.9-fold increase in the activity of NADPH (reduced form of nicotinamide adenine dinucleotide phosphate) oxidase, the major EC source of ROS, over its activity under baseline (normoxic) conditions (Fig. 3A). The NADPH oxidase activity of *Rac1*$^{+/-}$ ECs under H/R was comparable to that of *Rac1*$^{+/+}$ ECs under normoxic conditions, consistent with the known role of Rac1 as an activator of the NADPH oxidase complex (4). H/R caused a 1.6-fold increase in *Rac1*$^{+/+}$ ECs of the overall oxidative stress (OS), including hydrogen peroxide. OS of *Rac1*$^{+/-}$ ECs under H/R was substantially decreased compared to that of *Rac1*$^{+/+}$ ECs; indeed, OS of *Rac1*$^{+/-}$ ECs subjected to H/R was ~30% lower than that of *Rac1*$^{+/+}$ ECs at baseline. The decrease in OS in *Rac1*$^{+/-}$ ECs was more pronounced than the decrease in NADPH oxidase activity, suggesting the involvement of additional oxidoreductases, including Gpx3. In line

with the decrease in ROS and the increase in HSP abundance, apoptotic death of *Rac1*$^{+/-}$ ECs, at both baseline and H/R, was ~50% less than that of *Rac1*$^{+/+}$ ECs (Fig. 3B).

In the neurovascular unit, the basement membrane (BM) surrounds blood vessels and astrocyte endfeet and supports BBB integrity (2). In the early phases of stroke, the BM is attacked by proteases, such as matrix metalloproteinase 2 (MMP-2) and MMP-9 (3). Thus, enhancement of BM structure and function may help preserve BBB function. The ECM genes showing increased expression in *Rac1*$^{+/-}$ ECs included a subset that encodes BM constituents (Table 3 and table S4). These BM constituents are composed of structural [collagens (*Col2a1*, *Col8a1*), fibronectin (*Fn1*)] and regulatory proteins [thrombospondin 2 (*Thbs2*), osteopontin (*Spp1*)]. Additionally, a weak but coordinate increase in expression was noted for genes encoding perlecan [heparan sulfate proteoglycan 2 (*Hspg2*), 1.29-fold], collagens (*Col1a1*, 1.48-fold; *Col4a1*, 1.19-fold; *Col4a2*, 1.25-fold), thrombospondin 1 (*Thbs1*, 1.32-fold), and SPARC (secreted acidic cysteine-rich glycoprotein) (*Sparc*, 1.40-fold). Many of these proteins enhance collagen fibrillogenesis and matrix-cell adhesion, processes that stabilize the BM (26). Specifically, thrombospondin 1 and 2 bind to and inhibit MMP-2, a constitutively expressed protease that initiates the degradation of BM early in MCAo (3,26,27).

GSEA showed broad enrichment of *Rac1*$^{+/-}$ ECs in transforming growth factor–β (TGF-β)–responsive genes, including those encoding many ECM proteins (Fig. 2G and table S2). In the array data, the genes encoding TGF-β1−3 and TGF-β receptors 1 to 3 were not differentially expressed in *Rac1*$^{+/-}$ and *Rac1*$^{+/+}$ ECs; rather, genes encoding proteins that coordinately enhance activation of latent TGF-β complex, such as LTBP1 (latent TGF-β binding protein 1), LTBP3 (1.46-fold), thrombospondin 1, SPARC, and fibronectin, were enriched in *Rac1*$^{+/-}$ ECs (Table 3 and table S4) (28,29). Because TGF-β reportedly enhances neuronal survival and BBB function (2,30), the possible increase in the TGF-β signal may play a role in neuroprotection in EC-*Rac1*$^{+/-}$ mice.

Resistance of *Rac1*$^{+/-}$ ECs to hypoxia-induced endothelial permeability

The cell adhesion gene cluster also included genes encoding components of adherence junctions (protocadherin 10), desmosomes (desmocollin 3), and tight junctions (claudin 3, 1.35-fold) (Table 3 and table S4) (2). The increased abundance of BM and intercellular adhesion proteins in *Rac1*$^{+/-}$ ECs suggested that *Rac1*$^{+/-}$ EC monolayers would show a less permeable and dissociation-resistant phenotype. Indeed, maintenance of confluent *Rac1*$^{+/-}$ EC monolayers for more than 4 weeks reproducibly yielded firm cell sheets hardly dissociable with trypsin digestion (Fig. 3C). In contrast, *Rac1*$^{+/+}$ EC monolayers maintained under comparable conditions readily underwent dispersion by trypsin treatment. H/R increased the paracellular permeability of *Rac1*$^{+/+}$ ECs to horseradish peroxidase (HRP) 1.7-fold, but only affected that of *Rac1*$^{+/-}$ ECs minimally (Fig. 3D). *Rac1*$^{+/-}$ ECs showed additional features consistent with enhanced ability to act as a barrier: up-regulation of the gene encoding anti-edemagenic protein thrombospondin 2 (31) and the circumferential redistribution of F-actin together with a decrease in its abundance [a cytoskeletal change typically associated with reduced endothelial permeability (32)] (Fig. 4). The decrease in F-actin abundance in *Rac1*$^{+/-}$ ECs is consistent with the decrease in Rac1 and mDia2 (*Diap3*,Table 2), which cooperatively promote actin microfilament formation (6,33,34).

Leucocyte-EC adhesion is an important component of vascular injury in MCAo. However, the similar increase in monocyte adhesion (Fig. 3E) and vascular cell adhesion molecule–1 (VCAM-1) (Fig. 3F) mRNA abundance produced by H/R in *Rac1*$^{+/-}$ and *Rac1*$^{+/+}$ ECs argues against the involvement of this mechanism for the neuroprotection in EC-*Rac1*$^{+/-}$ mice. Overall, decreased Rac1 promotes the antioxidative, survival, and barrier properties of ECs, thereby imparting resistance to ischemic insult.

Rac1$^{+/-}$ ECs exert neuroprotection through paracrine mechanisms

The expression of genes encoding 13 growth factors was up-regulated in *Rac1*$^{+/-}$ ECs. Four of these growth factors [artemin, fibroblast growth factor 5 (FGF-5), bone morphogenetic protein 6 (BMP-6), and TGF-α] are endowed with potential neurotrophic capacity (Table 3) (35–39). The genes encoding these factors are expressed basally or inducibly in vascular endothelium and in the central nervous system (CNS). We first determined the mRNA abundance of these neurotrophic factors, along with that of crystallin αB, Gpx3, and thrombospondin 2, in EC-*Rac1*$^{+/-}$ and control whole mouse brains (Fig. 5A). Of these, artemin (4.5-fold), FGF-5 (1.4-fold), and Gpx3 (1.4-fold) were significantly up-regulated in the EC-*Rac1*$^{+/-}$ brain compared to control. All of the genes examined are reportedly expressed in nonvascular cells such as neurons and glia; thus, background expression would likely mask their possible local enrichment in the vascular endothelium of EC-*Rac1*$^{+/-}$ brain.

Given the enrichment of neurotrophic factors, we hypothesized that *Rac1*$^{+/-}$ ECs support neuronal survival through paracrine mechanisms. To address this question, we performed noncontiguous co-culture experiments in which ECs were grown on a porous insert over a compartment in which neuronal cells were cultured (Fig. 5B). *Rac1*$^{+/-}$ and *Rac1*$^{+/+}$ mouse ECs were grown to confluence on Transwell insert membranes with 0.4-μm pores, which allow passage of humoral factors to the lower compartment. After reaching confluence, ECs on inserts were co-cultivated with SH-SY5Y cells, a neuroblastoma cell line that expresses functional receptors to glial cell line–derived neurotrophic factor (GDNF) ligands, including artemin (35). After 2-day co-culture, SH-SY5Y cells left in conditioned media were exposed to hypoxic conditions for 24 hours. Hypoxia-induced apoptosis, as assessed by Annexin V labeling, was reduced in cells co-cultured with *Rac1*$^{+/-}$ ECs (14%) compared to those co-cultured with *Rac1*$^{+/+}$ ECs (26%), suggesting increased production of neurotrophic factors by *Rac1*$^{+/-}$ versus *Rac1*$^{+/+}$ ECs (Fig. 5C). To extend this finding, we focused on artemin, the most highly up-regulated neurotrophic factor in *Rac1*$^{+/-}$ ECs. Cortical neurons isolated from fetal mouse brain at around embryonic day 16 (E16) were co-cultured with mouse brain ECs (MBECs) derived from EC-*Rac1*$^{+/-}$ and control mice (Fig. 5B and fig S3). After 2-day co-culture, the neurons were challenged with 2-hour oxygen and glucose deprivation (OGD) followed by 22-hour reoxygenation (Fig. 5D). Administration of recombinant artemin (with blank inserts) elicited a dose-dependent inhibition of neuronal apoptosis, determined by the fraction of cells containing cleaved caspase 3. Endothelial co-culture attenuated neuronal apoptosis by 23% with control MBECs and by 52% with EC-*Rac1*$^{+/-}$ MBECs, indicating that EC secretion of neurotrophic factors is increased by *Rac1* haploinsufficiency. Next, we tested the effect of artemin-neutralizing antibody or control immunoglobulin G (IgG) in neuron-EC co-cultures. Artemin-neutralizing antibodies had little effect on neuroprotection by control MBECs, but reduced neuroprotection by EC-*Rac1*$^{+/-}$ MBECs by half. These results suggest that the potentiation of EC-derived neurotrophic activity by *Rac1* haploinsufficiency depends in part on increased production of artemin. The residual antiapoptotic activity that persists in the presence of artemin-neutralizing antibody implicates additional neurotrophic factors in the neurotrophic effects of EC-*Rac1*$^{+/-}$ MBECs.

DISCUSSION

We have shown that *Rac1* haploinsufficiency in ECs is neuroprotective through the release of neurotrophic factors. The neuroprotective mechanism is due, in part, to increased release of artemin from haploinsufficient *Rac1* ECs. Artemin is a member of the GDNF family of ligands (GFLs) that is expressed in various neural and nonneural tissues, including vascular walls (smooth muscle cells and ECs) (35,40,41). GFLs exert antiapoptotic signals on neurons by binding to a receptor complex composed of GDNF receptor α (GFRα) and RET (rearranged during transfection) proto-oncogene (8). The principal receptor for artemin is GFRα3, which

is expressed mainly in nonneural tissues and in the peripheral nervous system (42). Studies with mice lacking artemin uncovered its role as a vascular-derived guidance factor for sympathetic neuron axonal projections (40). In the CNS, artemin is expressed in low abundance during development and adulthood in distinct regions, such as the basal ganglia and thalamus, whereas GFRα3 expression is almost nonexistent (35,42). Despite the low abundance and restricted distribution of endogenous artemin in the CNS, administration of exogenous artemin potently promotes the survival of neurons from various CNS regions including midbrain dopaminergic neurons, cortical GABAergic neurons, and hippocampal neurons (43–45). Reportedly, artemin can also signal through GFRα1, which is the principal receptor for GDNF and shows widespread, ischemia-inducible CNS expression and neuroprotective capacity in MCAo (35,37,39). Therefore, we consider that the reduction in infarct size in EC-*Rac1*$^{+/-}$ mice was likely exerted through EC-derived artemin acting through the GFRα1 system.

The mechanism whereby inhibition of Rac1 leads to differential expression of the genes encoding a subset of neurotrophic factors is unclear. A recent study showed that integrin-linked kinase up-regulates brain-derived neurotrophic factor in ECs (13). Given that Rac1 is critical for outside-in signaling in response to cell adhesion, our observation that Rac1 insufficiency promotes the expression of ECM components and cell adhesion molecules may be pertinent to ECM regulation of neurotrophic activity in ECs.The TGF-β pathway may also play a role in up-regulating neurotrophic factors in *Rac1*$^{+/-}$ ECs, because the expression of artemin and TGF-α is reportedly inducible by TGF-β in pancreatic stellate cells and ECs (46,47).

In animal models of neurological diseases, neurotrophic factors show therapeutic potential when delivered locally by surgical procedures. In clinical application, less invasive delivery through blood flow and cerebrospinal fluid was ineffective because of the poor bioavailability at target tissues due, in part, to poor BBB penetration, low tissue diffusion, and short half-life (7–9). Moreover, administration of high-dose neurotrophic factors frequently led to adverse effects, because of their systemic, pleiotropic actions, and interference with normal brain functions. Therefore, augmentation of endogenous neurotrophic activity within the confines of the neurovascular unit could represent an alternative therapeutic strategy that circumvents many, if not all, of these hurdles. We showed that inhibition of EC Rac1 potentiated endothelial expression of neurotrophic factors severalfold. Small increases in neurotrophic factor production may be therapeutically efficacious, as suggested by a recent study showing that a threefold increase in the abundance of GDNF protein was effective in a primate model of Parkinson's disease (48).

Our data suggest that EC *Rac1* haploinsufficiency is neuroprotective through two mechanisms: It enhances vascular barrier integrity and independently promotes neuronal survival (Fig. 5E). Accumulating evidence indicates that targeting a single pathological process does not suffice for neuroprotection and points to the importance of combination therapies (49). In this regard, the multiple neuroprotective mechanisms potentially elaborated by *Rac1*$^{+/-}$ ECs may be beneficial. Considering the well-established roles of matrix-cell interaction in cell survival, increased expression of BM components may not only enhance BBB integrity, but also could directly contribute to preventing neuronal cell death. Indeed, fibronectin provides neuroprotection in mice MCAo (50). Conversely, the neurotrophic factors up-regulated in *Rac1*$^{+/-}$ ECs also have gliotrophic functions that could enhance the vascular barrier (2). For example, FGF-5 regulates the astrocyte endfeet coverage of blood vessels and enhances BBB function (51). Furthermore, it is becoming increasingly clear that cytokines that are ineffective in isolation can become neurotrophically active when acting together (30). The small but coordinate up-regulation of various growth factors in *Rac1*$^{+/-}$ ECs conforms to this notion and may underlie the neuroprotection seen in MCAo.

Because ECs represent a highly drug-accessible brain compartment, targeting endothelial Rac1 may provide a therapeutically feasible approach for intervention of the cross talk between ECM and cellular components within the neurovascular unit. The therapeutic time window of neurotrophic factor therapy for acute ischemic stroke is typically within 1 hour of reperfusion (37). Furthermore, BM disruption commences within hours of the stroke onset (3). Therefore, prophylactic inhibition of EC Rac1 may be beneficial for effective neuroprotection. However, Rac1 deletion in ECs could also lead to decreased angiogenic response (Supplementary text and fig. S2). It remains to be determined, therefore, what the effect of sustained inhibition of endothelial Rac1 is on neurogenesis, which is coupled to angiogenesis within the neurovascular niche (52,53).

In conclusion, our study provides a previously unexplored therapeutic strategy for neuroprotection by targeting EC signaling. Our study is somewhat limited by the examination of transcriptional profile of *Rac1* deletion in heart rather than brain ECs. However, our finding that EC-*Rac1*$^{+/-}$ mice showed a reduction in brain edema volume after ischemic stroke agrees with the notion that inhibition of Rac1 in brain ECs is protective of BBB function. Moreover, increased expression of the neurotrophic factor artemin was validated with *Rac1* deletion in brain ECs. In addition, expression of the genes encoding artemin and FGF-5, as well as that of the stress-related gene *Gpx3*, was up-regulated in whole brains of EC-*Rac1*$^{+/-}$ mice. Thus, the emerging possibility that paracrine signals from endothelium could have a global role in tissue differentiation (and organ formation and function) indicates the broad applicability of exploiting EC signals for therapies targeting adjacent parenchymal tissues (54).

MATERIALS AND METHODS

Expanded materials and methods are available in Supplementary Materials.

Generation of EC-*Rac1*$^{+/-}$ mice and the transient MCAo model

All animal protocols were approved by the Harvard Medical School's Standing Committee on Animal Welfare and Protection and are in accordance with the *Guide for the Care and Use of Laboratory Animals*, published by the National Institutes of Health. Male littermates (12 to 20 weeks) were used for experiments. *Rac1* conditional allele knock-in mice (*Rac1*$^{flox/flox}$) were developed as described (16) and crossed with Tie2-Cre Tg mice (Jackson Laboratory) (15) to generate EC-*Rac1*$^{+/-}$ (Tie2-Cre *Rac1*$^{flox/+}$) and control (*Rac1*$^{flox/+}$) mice. Transient MCAo and assessment of cerebral infarct volume, neurological deficit, and absolute CBF was conducted as described (17).

Isolation and culture of mouse primary ECs

Mouse primary ECs were isolated from heart as described (55), using an affinity selection method with Dynabeads conjugated with sheep antibody against rat IgG (Invitrogen), and rat antibodies against PECAM-1, and intercellular adhesion molecule–2 (ICAM2) (BD Biosciences). The cells were cultured in Dulbecco's modified Eagle's medium (DMEM) with 20% fetal calf serum (FCS), heparin, penicillin, streptomycin, and EC growth factor (ECGF). The preparation of *Rac1*$^{+/-}$ and *Rac1*$^{+/+}$ ECs was verified by guanosine triphosphate–Rac1 pull-down assay and immunoblotting with Rac1 (BD Biosciences) and actin (Sigma) antibodies.

Microarray and gene cluster analysis

Total RNA was prepared from subconfluent *Rac1*$^{+/-}$ and *Rac1*$^{+/+}$ mouse ECs at passage 4 through the sequential use of Trizol reagent (Invitrogen) and RNeasy columns (Qiagen). Complementary DNA (cDNA) labeling, hybridization, and image acquisition was performed at the Massachusetts General Hospital Microarray Core. The cDNA was reverse transcribed

from 8 μg of RNA, coupled to Cy3 or Cy5 dye, and hybridized in four replicates to a microarray containing 19,549 70-mer oligonucleotides. The fold ratio of *Rac1*$^{+/-}$ versus *Rac1*$^{+/+}$ for each reporter was statistically analyzed with one-sample Student's *t* test and Wilcoxon signed rank test and considered significant at $P < 0.05$. Reporters with the fold ratio of greater than 1.5 (up-regulated) or less than −1.5 (down-regulated) were considered differentially expressed and were uploaded onto DAVID 2007 (http://david.abcc.ncifcrf.gov/home.jsp) for gene annotation analysis (18). Enrichment of a given gene annotation was determined by EASE score, a modified Fisher's exact *P* value. Functional annotation clusters were determined by the degrees of gene co-association between annotation terms and were ranked by the Enrichment Score, the geometric mean (in –log scale) of member's EASE scores. To test for related genes systematically altered in *Rac1*$^{+/-}$ ECs, we used GSEA, a method that combines information from previously defined gene sets (www.broad.mit.edu/gsea/index.jsp) (19). Genes from the microarray were first ranked according to the expression difference (signal-to-noise ratio) between *Rac1*$^{+/-}$ and *Rac1*$^{+/+}$ ECs. The extent of association was then measured by a nonparametric running sum statistic. The complete set of microarray data is available at Gene Expression Omnibus (www.ncbi.nlm.nih.gov/geo/) with an accession number GSE15003.

Quantitative RT-PCR

Total RNA (50 to 100 ng) was used for real-time RT-PCR with a QuantiTect SYBR Green RT-PCR kit (Qiagen). The mRNA abundance was normalized with GAPDH mRNA or 18S ribosomal RNA.

Immunofluorescence

Mouse ECs were fixed with 3.7% paraformaldehyde, permeabilized with 0.1% Triton X-100, and probed with crystallin αB antibody (Stressgen) and Alexa488-conjugated secondary antibody (Molecular Probe). Images were acquired by a confocal microscope (Leica).

Assessment of oxidative stress

Hypoxic condition was introduced by modular chambers (Billups-Rothenberg) filled with 95% N_2 and 5% CO_2 at 37°C. After hypoxia, cells were returned to a regular incubator for reoxygenation (H/R). ECs were exposed to H/R (4 hours/2 hours) and treated with 3.3 μM lucigenin and 67 μM NADPH. The NADPH oxidase activity was determined as diphenylene iodonium (DPI)–inhibitable lucigenin chemiluminescence by a luminometer (PerkinElmer). Cells preloaded with 100 μM 2′,7′-dichlorofluorescein diacetate (DCFH-DA) were exposed to H/R and the OS was determined as DCF fluorescence by 485-nm excitation and 530-nm emission filters.

Annexin V binding assay

Cells were trypsinized, labeled with Annexin V-EGFP (10 μg/ml) in binding buffer containing 2.5 mM $CaCl_2$ for 15 min and analyzed by flow cytometry.

Assessment of cell adhesion and EC barrier function

Cell adhesion was assessed by the time required for obtaining single-cell suspensions in 0.25% trypsin/1 mM EDTA solution (Invitrogen) at 37°C. Confluent ECs on Transwell inserts (0.4-μm pore size) were treated with HRP (20 μg/ml) in the upper chamber, and the medium in the lower chamber was incubated in buffer (0.5 mM guaiacol, 50 mM Na_2HPO_4, and 0.6 mM H_2O_2) to assess the HRP activity that passed across the EC layer as absorbance at 470 nm.

Assessment of EC-leucocyte attachment

ECs were co-cultured with [^{3}H]thymidine-labeled THP-1 cells (10^6 cells/ml) for 3 hours. The adherent cells were lysed with 0.5 M NaOH and analyzed in a scintillation counter.

Isolation and culture of neuronal cells and MBECs

SH-SY5Y cells (American Type Culture Collection) were cultured in Eagle's minimum essential medium/F12 medium with 10% FCS. Cortical neurons were isolated from fetal mouse brains (~E16) with the use of trypsin and deoxyribonuclease I (DNase I) and plated at 10^5 cells/cm^2 on poly-D-lysine–coated coverslips in Neurobasal medium (Invitrogen) with 1 mM glutamine, 2% B27 supplement, and antibiotics. The medium was half changed every 3 days. For MBEC isolation, cortices from 6 to 10 adult mice were homogenized, deprived of lipid debris by centrifugation in 15% dextran (10,000g), and digested with Collagenase/Dispase (Roche) and DNase I. After centrifugation in 45% Percoll (20,000g), the top layer was plated in DMEM/F12 with 10% horse serum, 10% FCS, heparin, antibiotics, and ECGF.

EC-neuron co-culture and assessment of neuronal cell death

For co-culture, ECs grown on Transwell inserts (0.4-μm pore) were applied to neuronal cell cultures for 48 hours and thereafter removed. SH-SY5Y cells were exposed to 24-hour hypoxia, followed by Annexin V-EGFP labeling. The cortical neurons (day 14) were co-cultured with MBECs (passage 3) in the presence of vehicle, goat anti-mouse artemin-neutralizing antibody or goat IgG (0.5 μg/ml, R&D) in the lower compartment. Some neurons were treated with blank inserts and recombinant mouse artemin (0 to 10 ng/ml). After co-culture, the neurons were deprived of the conditioned media (CM), treated with glucose-free DMEM under hypoxia for 2 hours (OGD), and resupplied with the CM and reoxygenated for 22 hours. The neurons were immunostained with cleaved caspase-3 (Asp^{175}) (5A1) rabbit monoclonal antibody (Cell Signaling) overnight, and Alexa568-conjugated antibody against rabbit IgG and 4′,6-diamino-2-phenylindole (DAPI) for 1 hour.

Statistical analysis

Unless otherwise noted, all statistical analysis was carried out by analysis of variance (ANOVA) followed by Fisher's test. $P < 0.05$ was considered to be significant.

Supplementary Material

Refer to Web version on PubMed Central for supplementary material.

REFERENCES AND NOTES

1. Cheng T, Liu D, Griffin JH, Fernandez JA, Castellino F, Rosen ED, Fukudome K, Zlokovic BV. Activated protein C blocks p53-mediated apoptosis in ischemic human brain endothelium and is neuroprotective. Nat. Med 2003;9:338–342. [PubMed: 12563316]
2. Abbott NJ, Ronnback L, Hansson E. Astrocyte–endothelial interactions at the blood–brain barrier. Nat. Rev. Neurosci 2006;7:41–53. [PubMed: 16371949]
3. Cunningham LA, Wetzel M, Rosenberg GA. Multiple roles for MMPs and TIMPs in cerebral ischemia. Glia 2005;50:329–339. [PubMed: 15846802]
4. Gregg D, Rauscher FM, Goldschmidt-Clermont PJ. Rac regulates cardiovascular superoxide through diverse molecular interactions: More than a binary GTP switch. Am. J. Physiol. Cell Physiol 2003;285:C723–C734. [PubMed: 12958025]
5. Tzima E. Role of small GTPases in endothelial cytoskeletal dynamics and the shear stress response. Circ. Res 2006;98:176–185. [PubMed: 16456110]
6. Etienne-Manneville S, Hall A. Rho GTPases in cell biology. Nature 2002;420:629–635. [PubMed: 12478284]

7. Pardridge WM. Drug and gene delivery to the brain: The vascular route. Neuron 2002;36:555–558. [PubMed: 12441045]
8. Bespalov MM, Saarma M. GDNF family receptor complexes are emerging drug targets. Trends Pharmacol. Sci 2007;28:68–74. [PubMed: 17218019]
9. Wu D. Neuroprotection in experimental stroke with targeted neurotrophins. NeuroRx 2005;2:120–128. [PubMed: 15717063]
10. Zlokovic BV. The blood-brain barrier in health and chronic neurodegenerative disorders. Neuron 2008;57:178–201. [PubMed: 18215617]
11. Lo EH, Dalkara T, Moskowitz MA. Mechanisms, challenges and opportunities in stroke. Nat. Rev. Neurosci 2003;4:399–415. [PubMed: 12728267]
12. Leventhal C, Rafii S, Rafii D, Shahar A, Goldman SA. Endothelial trophic support of neuronal production and recruitment from the adult mammalian subependyma. Mol. Cell. Neurosci 1999;13:450–464. [PubMed: 10383830]
13. Guo S, Kim WJ, Lok J, Lee SR, Besancon E, Luo BH, Stins MF, Wang X, Dedhar S, Lo EH. Neuroprotection via matrix-trophic coupling between cerebral endothelial cells and neurons. Proc. Natl. Acad. Sci. U.S.A 2008;105:7582–7587. [PubMed: 18495934]
14. Sawada N, Salomone S, Kim HH, Kwiatkowski DJ, Liao JK. Regulation of endothelial nitric oxide synthase and postnatal angiogenesis by Rac1. Circ. Res 2008;103:360–368. [PubMed: 18599867]
15. Koni PA, Joshi SK, Temann UA, Olson D, Burkly L, Flavell RA. Conditional vascular cell adhesion molecule 1 deletion in mice: Impaired lymphocyte migration to bone marrow. J. Exp. Med 2001;193:741–754. [PubMed: 11257140]
16. Glogauer M, Marchal CC, Zhu F, Worku A, Clausen BE, Foerster I, Marks P, Downey GP, Dinauer M, Kwiatkowski DJ. Rac1 deletion in mouse neutrophils has selective effects on neutrophil functions. J. Immunol 2003;170:5652–5657. [PubMed: 12759446]
17. Kim HH, Sawada N, Soydan G, Lee HS, Zhou Z, Hwang SK, Waeber C, Moskowitz MA, Liao JK. Additive effects of statin and dipyridamole on cerebral blood flow and stroke protection. J. Cereb. Blood Flow Metab 2008;28:1285–1293. [PubMed: 18382469]
18. Dennis G Jr. Sherman BT, Hosack DA, Yang J, Gao W, Lane HC, Lempicki RA. DAVID: Database for Annotation, Visualization, and Integrated Discovery. Genome Biol 2003;4:P3. [PubMed: 12734009]
19. Subramanian A, Tamayo P, Mootha VK, Mukherjee S, Ebert BL, Gillette MA, Paulovich A, Pomeroy SL, Golub TR, Lander ES, Mesirov JP. Gene set enrichment analysis: A knowledge-based approach for interpreting genome-wide expression profiles. Proc. Natl. Acad. Sci. U.S.A 2005;102:15545–15550. [PubMed: 16199517]
20. Olson MF, Ashworth A, Hall A. An essential role for Rho, Rac, and Cdc42 GTPases in cell cycle progression through G1. Science 1995;269:1270–1272. [PubMed: 7652575]
21. Bierl C, Voetsch B, Jin RC, Handy DE, Loscalzo J. Determinants of human plasma glutathione peroxidase (GPx-3) expression. J. Biol. Chem 2004;279:26839–26845. [PubMed: 15096516]
22. Voetsch B, Jin RC, Bierl C, Benke KS, Kenet G, Simioni P, Ottaviano F, Damasceno BP, Annichino-Bizacchi JM, Handy DE, Loscalzo J. Promoter polymorphisms in the plasma glutathione peroxidase (*GPx-3*) gene: A novel risk factor for arterial ischemic stroke among young adults and children. Stroke 2007;38:41–49. [PubMed: 17122425]
23. Gabai VL, Sherman MY. Invited review: Interplay between molecular chaperones and signaling pathways in survival of heat shock. J. Appl. Physiol 2002;92:1743–1748. [PubMed: 11896044]
24. Kamradt MC, Chen F, Sam S, Cryns VL. The small heat shock protein αB-crystallin negatively regulates apoptosis during myogenic differentiation by inhibiting caspase-3 activation. J. Biol. Chem 2002;277:38731–38736. [PubMed: 12140279]
25. Beere HM. Stressed to death: Regulation of apoptotic signaling pathways by the heat shock proteins. Sci. STKE 2001;2001:RE1. [PubMed: 11752668]
26. Bornstein P, Agah A, Kyriakides TR. The role of thrombospondins 1 and 2 in the regulation of cell-matrix interactions, collagen fibril formation, and the response to injury. Int. J. Biochem. Cell Biol 2004;36:1115–1125. [PubMed: 15094126]
27. Bornstein P. Thrombospondins as matricellular modulators of cell function. J. Clin. Invest 2001;107:929–934. [PubMed: 11306593]

28. Murphy-Ullrich JE, Poczatek M. Activation of latent TGF-beta by thrombospondin-1: Mechanisms and physiology. Cytokine Growth Factor Rev 2000;11:59–69. [PubMed: 10708953]
29. Dallas SL, Sivakumar P, Jones CJ, Chen Q, Peters DM, Mosher DF, Humphries MJ, Kielty CM. Fibronectin regulates latent transforming growth factor-β (TGFβ) by controlling matrix assembly of latent TGFβ-binding protein-1. J. Biol. Chem 2005;280:18871–18880. [PubMed: 15677465]
30. Unsicker K, Krieglstein K. Co-activation of TGF-ss and cytokine signaling pathways are required for neurotrophic functions. Cytokine Growth Factor Rev 2000;11:97–102. [PubMed: 10708957]
31. Lange-Asschenfeldt B, Weninger W, Velasco P, Kyriakides TR, von Andrian UH, Bornstein P, Detmar M. Increased and prolonged inflammation and angiogenesis in delayed-type hypersensitivity reactions elicited in the skin of thrombospondin-2–deficient mice. Blood 2002;99:538–545. [PubMed: 11781236]
32. Dudek SM, Garcia JG. Cytoskeletal regulation of pulmonary vascular permeability. J. Appl. Physiol 2001;91:1487–1500. [PubMed: 11568129]
33. Guo F, Debidda M, Yang L, Williams DA, Zheng Y. Genetic deletion of Rac1 GTPase reveals its critical role in actin stress fiber formation and focal adhesion complex assembly. J. Biol. Chem 2006;281:18652–18659. [PubMed: 16698790]
34. Harris ES, Rouiller I, Hanein D, Higgs HN. Mechanistic differences in actin bundling activity of two mammalian formins, FRL1 and mDia2. J. Biol. Chem 2006;281:14383–14392. [PubMed: 16556604]
35. Baloh RH, Tansey MG, Lampe PA, Fahrner TJ, Enomoto H, Simburger KS, Leitner ML, Araki T, Johnson EM Jr. Milbrandt J. Artemin, a novel member of the GDNF ligand family, supports peripheral and central neurons and signals through the GFRα3-RET receptor complex. Neuron 1998;21:1291–1302. [PubMed: 9883723]
36. Reuss B, von Bohlen und Halbach O. Fibroblast growth factors and their receptors in the central nervous system. Cell Tissue Res 2003;313:139–157. [PubMed: 12845521]
37. Harvey BK, Hoffer BJ, Wang Y. Stroke and TGF-β proteins: Glial cell line–derived neurotrophic factor and bone morphogenetic protein. Pharmacol. Ther 2005;105:113–125. [PubMed: 15670622]
38. Junier MP. What role(s) for TGFα in the central nervous system? Prog. Neurobiol 2000;62:443–473. [PubMed: 10869779]
39. Wang Y, Chang CF, Morales M, Chiang YH, Hoffer J. Protective effects of glial cell line–derived neurotrophic factor in ischemic brain injury. Ann. N. Y. Acad. Sci 2002;962:423–437. [PubMed: 12076993]
40. Honma Y, Araki T, Gianino S, Bruce A, Heuckeroth R, Johnson E, Milbrandt J. Artemin is a vascular-derived neurotropic factor for developing sympathetic neurons. Neuron 2002;35:267–282. [PubMed: 12160745]
41. Damon DH, Teriele JA, Marko SB. Vascular-derived artemin: A determinant of vascular sympathetic innervation? Am. J. Physiol. Heart Circ. Physiol 2007;293:H266–H273. [PubMed: 17337595]
42. Baloh RH, Gorodinsky A, Golden JP, Tansey MG, Keck CL, Popescu NC, Johnson EM Jr. Milbrandt J. GFRα3 is an orphan member of the GDNF/neurturin/persephin receptor family. Proc. Natl. Acad. Sci. U.S.A 1998;95:5801–5806. [PubMed: 9576965]
43. Rosenblad C, Grønborg M, Hansen C, Blom N, Meyer M, Johansen J, Dagø L, Kirik D, Patel UA, Lundberg C, Trono D, Björklund A, Johansen TE. *In vivo* protection of nigral dopamine neurons by lentiviral gene transfer of the novel GDNF-family member neublastin/artemin. Mol. Cell. Neurosci 2000;15:199–214. [PubMed: 10673327]
44. Ducray A, Krebs SH, Schaller B, Seiler RW, Meyer M, Widmer HR. GDNF family ligands display distinct action profiles on cultured GABAergic and serotonergic neurons of rat ventral mesencephalon. Brain Res 2006;1069:104–112. [PubMed: 16380100]
45. Bonde C, Kristensen BW, Blaabjerg M, Johansen TE, Zimmer J, Meyer M. GDNF and neublastin protect against NMDA-induced excitotoxicity in hippocampal slice cultures. Neuroreport 2000;11:4069–4073. [PubMed: 11192630]
46. Ceyhan GO, Bergmann F, Kadihasanoglu M, Erkan M, Park W, Hinz U, Giese T, Müller MW, Büchler MW, Giese NA, Friess H. The neurotrophic factor artemin influences the extent of neural damage and growth in chronic pancreatitis. Gut 2007;56:534–544. [PubMed: 17047099]

47. Viñals F, Pouysségur J. Transforming growth factor β1 (TGF-β1) promotes endothelial cell survival during in vitro angiogenesis via an autocrine mechanism implicating TGF-α signaling. Mol. Cell. Biol 2001;21:7218–7230. [PubMed: 11585905]

48. Eslamboli A, Georgievska B, Ridley RM, Baker HF, Muzyczka N, Burger C, Mandel RJ, Annett L, Kirik D. Continuous low-level glial cell line–derived neurotrophic factor delivery using recombinant adeno-associated viral vectors provides neuroprotection and induces behavioral recovery in a primate model of Parkinson's disease. J. Neurosci 2005;25:769–777. [PubMed: 15673656]

49. White BC, Sullivan JM, DeGracia DJ, O'Neil BJ, Neumar RW, Grossman LI, Rafols JA, Krause GS. Brain ischemia and reperfusion: Molecular mechanisms of neuronal injury. J. Neurol. Sci 2000;179:1–33. [PubMed: 11054482]

50. Sakai T, Johnson KJ, Murozono M, Sakai K, Magnuson MA, Wieloch T, Cronberg T, Isshiki A, Erickson HP, Fässler R. Plasma fibronectin supports neuronal survival and reduces brain injury following transient focal cerebral ischemia but is not essential for skin-wound healing and hemostasis. Nat. Med 2001;7:324–330. [PubMed: 11231631]

51. Reuss B, Dono R, Unsicker K. Functions of fibroblast growth factor (FGF)–2 and FGF-5 in astroglial differentiation and blood-brain barrier permeability: Evidence from mouse mutants. J. Neurosci 2003;23:6404–6412. [PubMed: 12878680]

52. Palmer TD, Willhoite AR, Gage FH. Vascular niche for adult hippocampal neurogenesis. J. Comp. Neurol 2000;425:479–494. [PubMed: 10975875]

53. Shen Q, Goderie SK, Jin L, Karanth N, Sun Y, Abramova N, Vincent P, Pumiglia K, Temple S. Endothelial cells stimulate self-renewal and expand neurogenesis of neural stem cells. Science 2004;304:1338–1340. [PubMed: 15060285]

54. Cleaver O, Melton DA. Endothelial signaling during development. Nat. Med 2003;9:661–668. [PubMed: 12778164]

55. Lim YC, Garcia-Cardena G, Allport JR, Zervoglos M, Connolly AJ, Gimbrone MA Jr. Luscinskas FW. Heterogeneity of endothelial cells from different organ sites in T-cell subset recruitment. Am. J. Pathol 2003;162:1591–1601. [PubMed: 12707043]

56. We thank D. J. Kwiatkowski for providing us with conditional Rac1 mice. This work was supported by grants from the NIH (HL052233, HL080187, and NS101828). N.S. was supported by the fellowships from the Uehara Memorial Foundation, the Cell Science Research Foundation, and Mochida Memorial Foundation for Medical and Pharmaceutical Research. There are no disclosures or conflicts of interest for all of the authors.

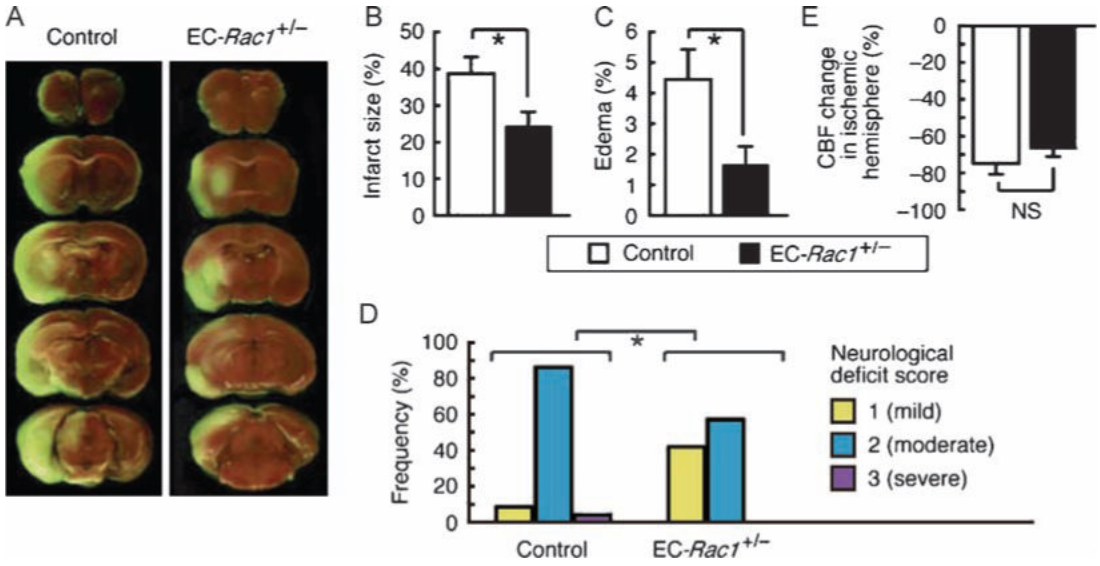

Fig. 1.

Haploinsufficiency of endothelial *Rac1* in mice leads to neuroprotection. EC-*Rac1*$^{+/-}$ and control mice underwent 2-hour MCAo followed by 22-hour reperfusion. (**A**) Representative brain sections stained with 2,3,5-triphenyltetrazolium chloride visualizing the infarct area. (**B** and **C**) Infarct (B) and edema (C) volumes of the ischemic hemisphere. (**D**) Neurological deficit score (n = 19 to 23 mice; *P < 0.05, Mann-Whitney test). (**E**) Change in CBF in the ischemic hemisphere at the end of 2-hour MCAo. (B, C, and E) Values are percent of the nonischemic hemisphere and shown as means ± SEM of 7 to 10 mice (*P < 0.05, ANOVA). NS, not significant.

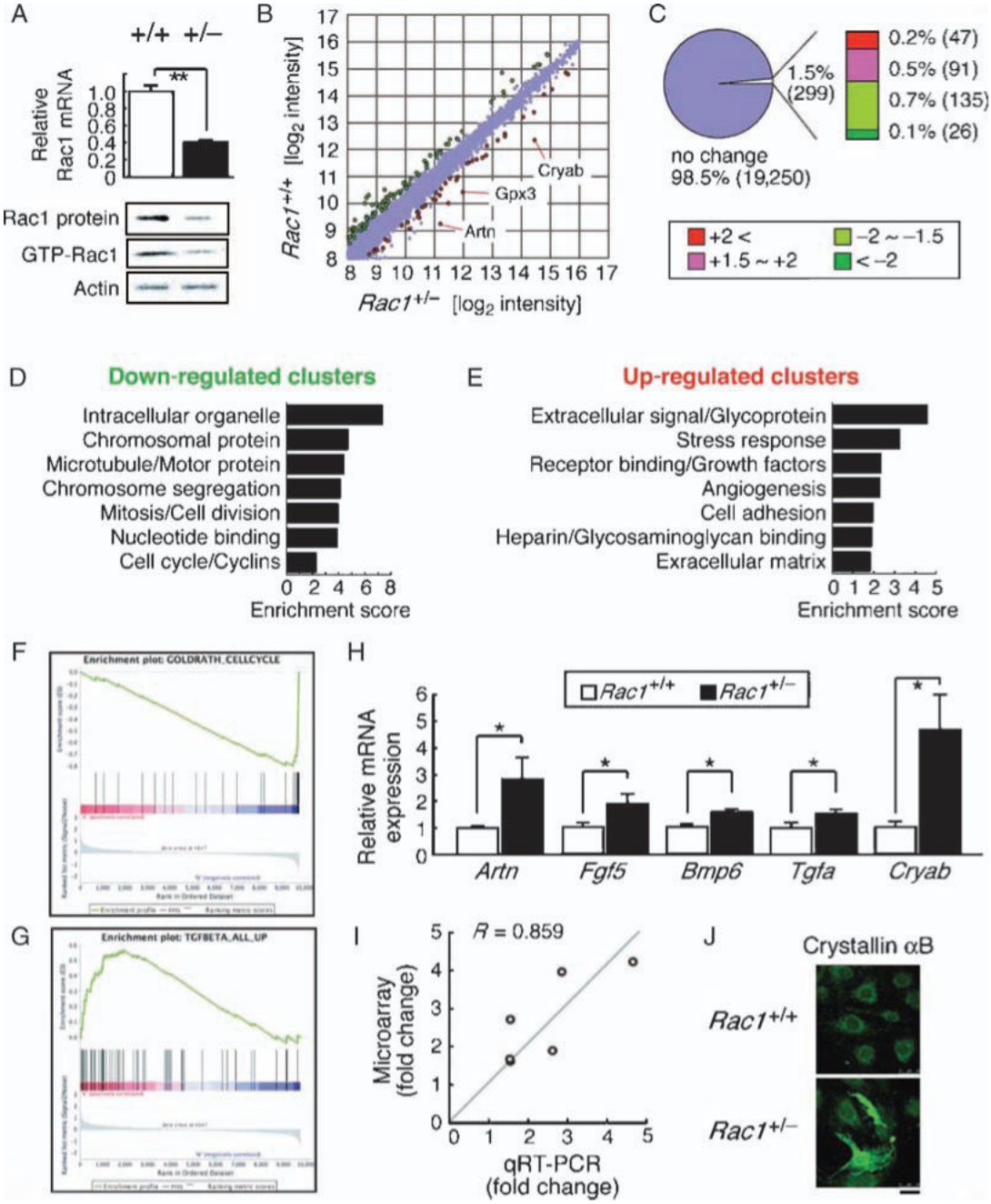

Fig. 2.

Expression profiling of *Rac1*$^{+/-}$ ECs. Differential mRNA expression between *Rac1*$^{+/-}$ and *Rac1*$^{+/+}$ mouse ECs was explored by microarray analysis. (**A**) qRT-PCR, immunoblotting, and GST-PAK (glutathione *S*-transferase–p21-activated protein kinase) pull-down assays showing Rac1 expression and activity in *Rac1*$^{+/-}$ and *Rac1*$^{+/+}$ ECs. (**B** and **C**) The up-regulated (red) and down-regulated (green) genes in *Rac1*$^{+/-}$ ECs. The scatter plot (B) shows 12,089 gene features with the signal intensity >200. (**D** and **E**) Functional annotation clustering of the down-regulated (D) and up-regulated (E) genes. (**F** and **G**) GSEA showing enrichment of cell cycle–related genes in *Rac1*$^{+/+}$ (F) and TGF-β–inducible genes in *Rac1*$^{+/-}$ ECs (G). Each plot displays (top) progression of the running enrichment score; (middle) "hits" in the gene set against the

ranked list of all genes in the data; (bottom) histogram for the ranked list. (**H** and **I**) qRT-PCR (H) and correlation analysis (I) to validate the microarray data. (**J**) Crystallin αB immunostaining of *Rac1*$^{+/-}$ versus *Rac1*$^{+/+}$ ECs. Scale bar, 25 μm. Values are means ± SEM of three to four replicates (*$P < 0.05$, **$P < 0.01$; ANOVA).

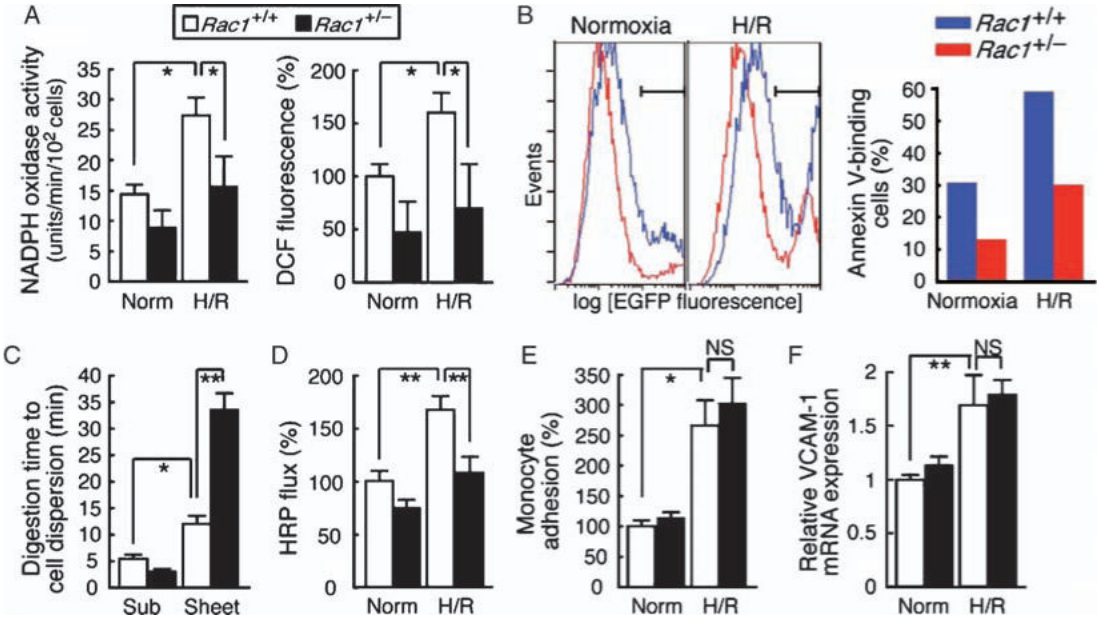

Fig. 3.

Phenotypic profiling of *Rac1*$^{+/-}$ ECs. (**A, B, D, E**, and **F**) *Rac1*$^{+/+}$ and *Rac1*$^{+/-}$ mouse ECs were sequentially exposed to 4-hour hypoxia and 2-hour (A and D) or 20-hour (B, E, and F) reoxygenation (H/R) or treated with normoxia (Norm). (A) NADPH oxidase activity (left) and ROS production (right) as determined by DPI-inhibitable lucigenin chemiluminescence and DCF fluorescence, respectively. (B) Apoptotic death was assessed by flow cytometry (left) as the Annexin V–EGFP–labeled EC fraction (right). (C)ECs at subconfluence (Sub) or prolonged confluence (>4 weeks) (Sheet) were subjected to standard trypsinization until single-cell suspensions were obtained. (D) The permeability of confluent EC monolayers grown on 0.4-μm Transwell inserts was assessed as HRP leak across the membrane during normoxia and H/R. (E) After exposure to normoxia or H/R, ECs were co-cultured with [^{3}H]thymidine-labeled monocytes (THP-1) for 3 hours. After washing, monocyte-EC binding was assessed as the cell lysate radioactivity. (F) VCAM-1 mRNA abundance was determined by qRT-PCR. (A, C to F) Values are means ± SEM of triplicates (*P < 0.05, **P < 0.01; ANOVA).

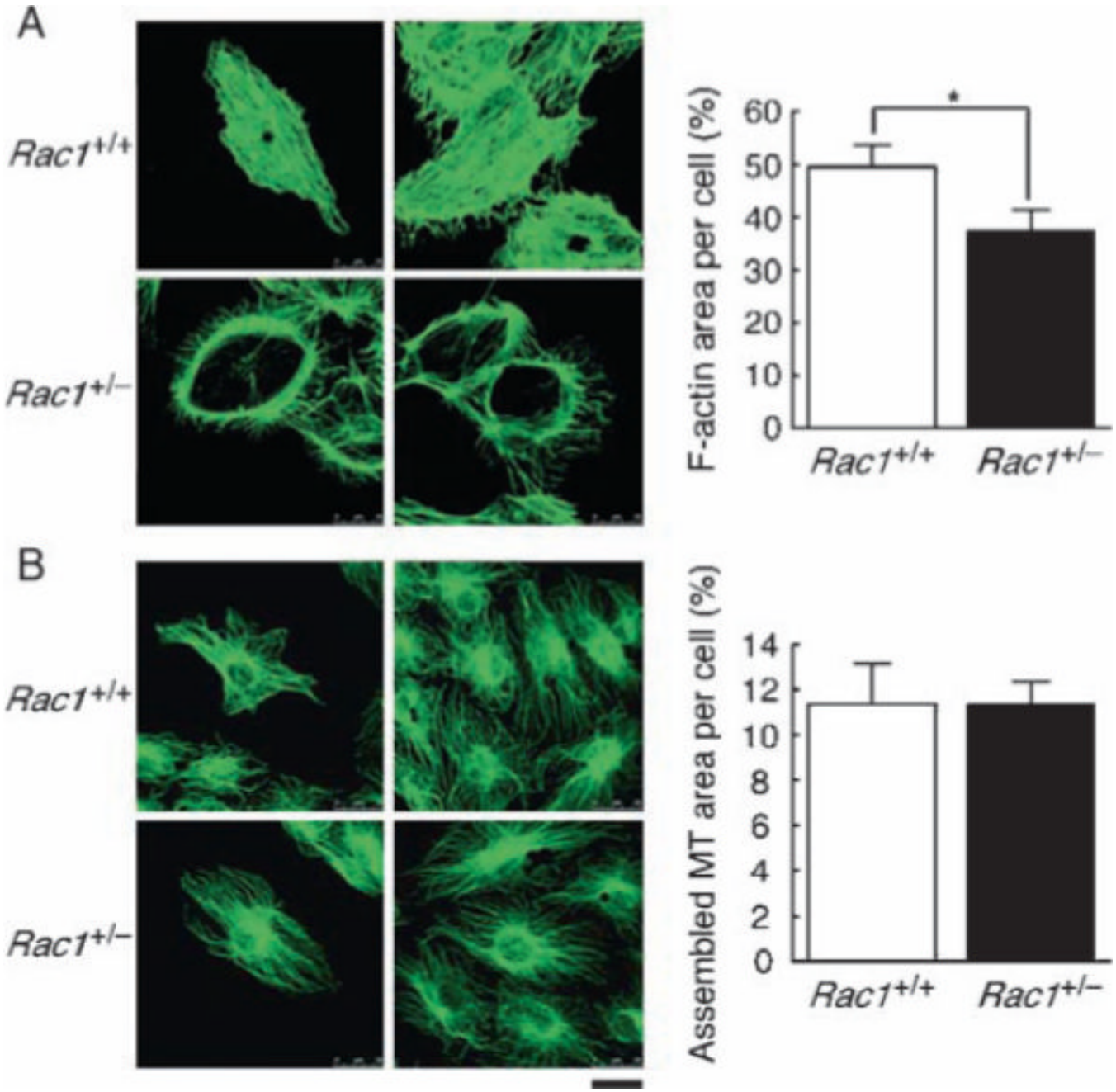

Fig. 4.

Decreased actin polymerization and circumferential redistribution of F-actin to the cortical areas in *Rac1*$^{+/-}$ ECs. Mouse ECs cultured in the presence of 20% serum were fixed and stained with (**A**) phalloidin to visualize F-actin and (**B**) antibody against β-tubulin for microtubules (MT). The F-actin and MT-labeled areas were quantified and represented as percent of total cell areas. Scale bar, 25 μm. Values are means ± SEM of five to seven replicates (*$P < 0.05$; ANOVA).

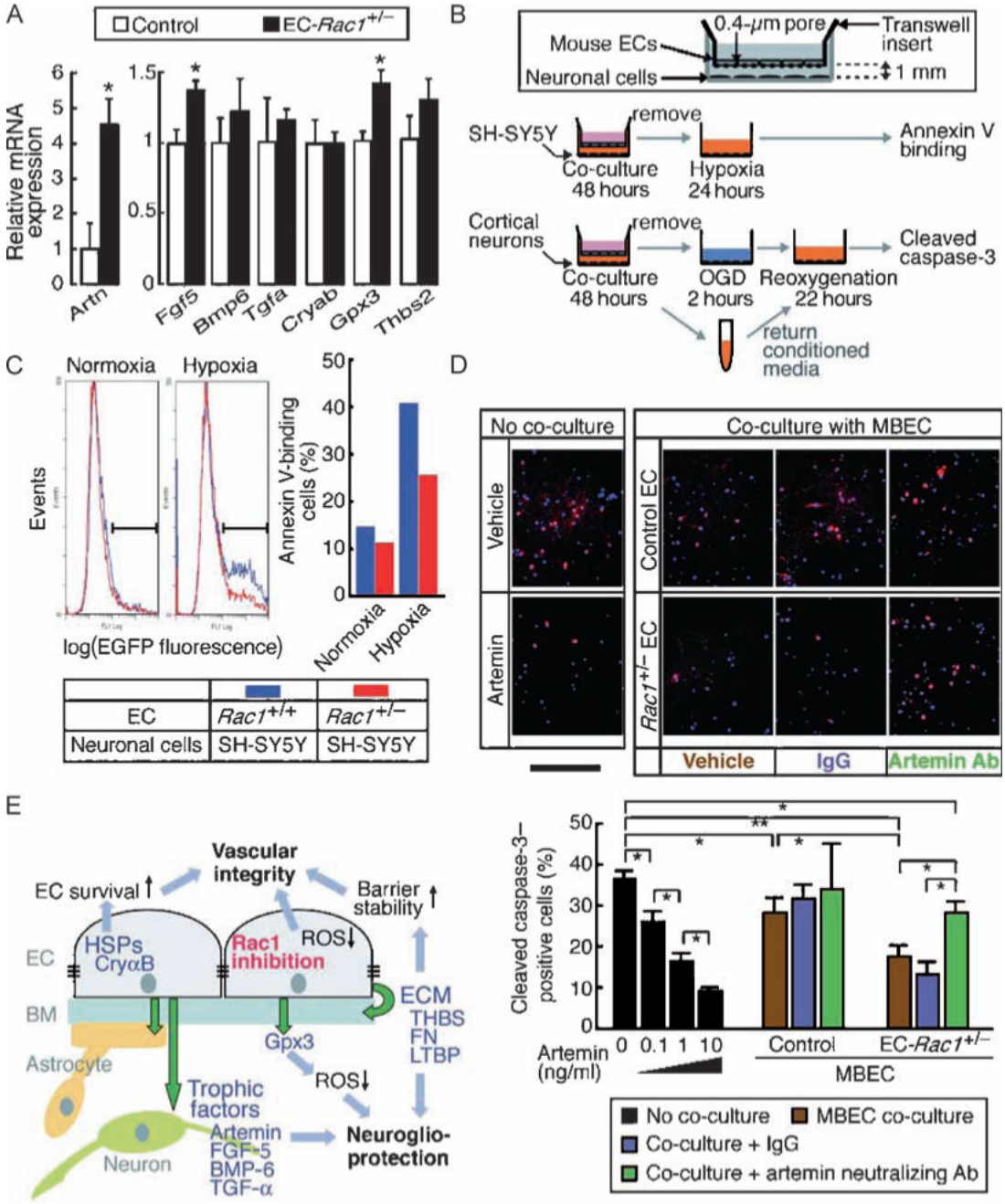

Fig. 5.

Rac1$^{+/-}$ ECs show enhanced neurotrophic activity through paracrine mechanisms. (**A**) mRNA expression of the potential neurotrophic factors was assessed in the EC-*Rac1*$^{+/-}$ and control mouse whole brains by qRT-PCR ($n = 7$ mouse brains). (**B**) Schematic of EC-neuron co-culture. (**C**) Co-culture with *Rac1*$^{+/-}$ versus *Rac1*$^{+/+}$ ECs mitigates hypoxia-induced apoptotic death of SH-SY5Y cells, as assessed by Annexin V-EGFP labeling and flow cytometry. (**D**) Cortical neurons isolated from fetal mouse brains (~E16) were co-cultured with EC-*Rac1*$^{+/-}$ or control MBECs in the presence of artemin-neutralizing antibody (Ab), control IgG, or vehicle in the lower chamber. Control neurons were treated with blank inserts and recombinant artemin proteins. Upper panel, after OGD and reoxygenation, the neurons were double-labeled with DAPI (blue) and cleaved caspase 3 (red). Scale bar, 1 mm. Lower panel, quantification of the

cleaved caspase 3–positive fractions. (**E**) A proposed model of neuroprotection through targeting endothelial Rac1. Values are means ± SEM (*$P < 0.05$, **$P < 0.01$; ANOVA).

Table 1

Hemodynamic profile and arterial blood gas analysis. MABP, mean arterial blood pressure; rCBF (regional cerebral blood flow) and blood gas were measured under inhalation anesthesia in the MCAo perioperative period. Pre, before MCAo; Post, after MCAo; $Paco_2$, partial pressure of arterial CO_2; Pao_2, partial pressure of arterial O_2. Control, n = 7 mice; EC-*Rac1*$^{+/-}$, n = 6 mice.

Hemodynamic parameter	Control	EC-*Rac1*$^{+/-}$
MABP (mmHg)		
Pre	91.1 ± 4.3	99.8 ± 3.2
Post	95.8 ± 6.0	102.1 ± 5.0
rCBF (%)		
Pre	102.6 ± 2.5	102.6 ± 1.5
MCAo	8.3 ± 1.1	6.0 ± 1.0
pH (arterial)		
Pre	7.40 ± 0.01	7.37 ± 0.04
MCAo	7.29 ± 0.02	7.25 ± 0.04
Post	7.28 ± 0.03	7.23 ± 0.03
$Paco_2$ (mmHg)		
Pre	29.3 ± 1.1	30.4 ± 3.5
MCAo	32.9 ± 3.2	35.5 ± 3.5
Post	48.6 ± 4.4	51.9 ± 4.2
Pao_2 (mmHg)		
Pre	120.6 ± 6.9	120.3 ± 16.9
MCAo	124.9 ± 9.2	127.5 ± 12.7
Post	127.1 ± 13.1	119.6 ± 7.1

Table 2

Selected genes down-regulated in *Rac1*$^{+/-}$ mouse ECs. Genes are categorized by the GO annotation.

Symbol	Gene name	Fold
	Cell cycle	
Fos	FBJ osteosarcoma oncogene	−3.02
Myb	Myeloblastosis oncogene	−1.57
Cdc2a	Cell division cycle 2 homolog A (*Schizosaccharomyces pombe*)	−2.11
Ccnb2	Cyclin B2	−1.88
Ccna2	Cyclin A2	−1.59
Nek2	NIMA (never in mitosis gene a)–related expressed kinase 2	−1.85
Mad2l1	MAD2 (mitotic arrest deficient, homolog)–like 1 (yeast)	−1.60
Cdca5	Cell division cycle associated 5	−1.54
Stk6	Aurora kinase A	−1.64
Tacc3	Transforming, acidic coiled-coil containing protein 3	−1.93
Bard1	BRCA1 associated RING domain 1	−1.57
Gadd45g	Growth arrest and DNA-damage–inducible 45 gamma	−1.70
Ect2	ect2 oncogene	−1.65
Mki67	Ki-67	−2.23
	Cytoskeleton organization and biogenesis	
Kif2c	Kinesin family member 2C	−1.65
Kif11	Kinesin-related mitotic motor protein	−2.05
Kif18a	Kinesin family member 18A	−1.74
Kif20a	Kinesin family member 20A	−1.76
Kif20b	Kinesin family member 20B	−1.73
Kif22	Kinesin family member 22	−1.58
Kif23	Kinesin family member 23	−1.59
Tpx2	TPX2, microtubule-associated protein homolog (*Xenopus laevis*)	−1.75
Birc5	Baculoviral IAP repeat–containing 5, survivin	−1.59
Mapt	Microtubule-associated protein tau	−2.06
Tubb6	Tubulin, beta6	−1.57
Pfn3	Profilin3	−1.58
Diap3	Diaphanous homolog 3	−1.97
	Chromosome organization and biogenesis	
Hist1h1a	Histone 1, H1A	−1.77
Hist1h1b	Histone 1, H1B	−1.99
Hist1h2ab	Histone 1, H2AB	−1.57
Hist2h2aa1	Histone 2, H2AA1	−1.52
Hist1h2bb	Histone 1, H2BB	−1.74
Hist2h2bb	Histone 2, H2BB	−1.73
Hist1h3f	Histone 1, H3F	−1.83
Hist1h3g	Histone 1, H3G	−1.94
Hmgb2	High-mobility group box 2	−1.52
Top2a	Topoisomerase (DNA) II alpha	−1.87

Symbol	Gene name	Fold

Table 3

Selected genes up-regulated in *Rac1*$^{+/-}$ mouse ECs. Genes are categorized by the GO annotation.

Symbol	Gene name	Fold
	Receptor binding	
Artn	Artemin	3.97
Fgf5	Fibroblast growth factor 5	2.73
Cxcl2	Chemokine (C-X-C motif) ligand 2	1.93
Fgf14	Fibroblast growth factor 14	1.91
Bmp6	Bone morphogenetic protein 6	1.82
Npy	Neuropeptide Y	1.69
Tgfa	Transforming growth factor alpha	1.68
Frs3	Fibroblast growth factor receptor substrate 3	1.55
Edn1	Endothelin 1	1.54
Nts	Neurotensin	1.53
	Cell surface receptor–linked signal transduction	
Crhr2	Corticotropin releasing hormone receptor 2	2.00
Adcy7	Adenylate cyclase 7	1.63
Robo4	Roundabout homolog 4 (*Drosophila*)	1.58
Cxcr4	Chemokine (C-X-C MOTIF) receptor 4	1.56
Ltbp1	Latent transforming growth factor beta binding protein 1	1.55
Adamts1	A disintegrin-like and metallopeptidase (reprolysin type) with thrombospondin type 1 motif, 1	1.52
	Response to stimulus	
Cryab	Crystallin, alpha B	4.24
Gpx3	Glutathione peroxidase 3	2.86
Hspb1	Heat shock protein 1 (hsp25)	1.68
Hspa1a	Heat shock protein 1B (hsp70)	1.62
	Cell adhesion	
Dsc3	Desmocollin 3	2.85
Pcdh10	Protocadherin 10	2.18
Col2a1	Procollagen, type II, alpha 1	1.74
Col8a1	Procollagen, type VIII, alpha 1	1.53
Fn1	Fibronectin 1	1.64
Thbs2	Thrombospondin 2	1.68
Spp1	Osteopontin	1.52